

Received: 2017.09.07
Accepted: 2018.04.24
Published: 2018.10.09

Clinical Value and Diagnostic Accuracy of 3.0T Multi-Parameter Magnetic Resonance Imaging in Traumatic Brachial Plexus Injury

Authors' Contribution:
Study Design A
Data Collection B
Statistical Analysis C
Data Interpretation D
Manuscript Preparation E
Literature Search F
Funds Collection G

BE 1 Lihong Zhang*
B 1 Taixing Xiao*
D 2 Qiufeng Yu
F 1 Yong Li
AG 3 Feng Shen
C 4 Wenming Li

1 The Medical Imaging Center, The Third People's Hospital of Liaocheng, Liaocheng, Shandong, P.R. China
2 The Magnetic Resonance Imaging Department, The Third People's Hospital of Liaocheng, Liaocheng, Shandong, P.R. China
3 Department of Radiology, Liaocheng People's Hospital, Liaocheng, Shandong, P.R. China
4 Technical Squadron of Criminal Investigation Brigade of Dongchang Fu Public Security Bureau, Liaocheng, Shandong, P.R. China

* These authors contribute equally to this work

Corresponding Author: Feng Shen, e-mail: shenfeng1963ryh@126.com
Source of support: Departmental sources

Background: The aim of this study was to evaluate the clinical value and diagnostic accuracy of 3.0T multi-parameter magnetic resonance imaging (MRI) in traumatic brachial plexus injury.


Material/Methods: Twenty-five healthy volunteers and 28 patients with clinically confirmed traumatic brachial plexus injury were enrolled in this study. Bilateral brachial plexus imaging was performed using conventional sequences (T1WI, T2WI), short time inversion recovery (STIR), balanced fast field echo (balance-FFE), and diffusion weighted imaging with background suppression (DWIBS). The MRI diagnosis was compared with intraoperative electromyography and surgery.

Results: Brachial plexus injuries were classified based on the anatomic locations. There were 16 patients with pre-ganglionic injury and 12 patients with post-ganglionic injury. The pre-ganglionic injury included ruptured nerve roots, stiff nerve roots, traumatic meningeal cysts, black line sign, spinal cord edema, and thickened nerve root sleeve. The post-ganglionic injury included thickened nerve roots, disappearance of normal nerve root structure or disrupted continuity of the nerve, stiff nerve roots, pseudo-neuroma, and abnormalities in the adjacent soft tissues. Comparing the results from MRI and surgery, the sensitivity, specificity, and accuracy of MRI examination were 93.55%, 71.43%, and 89.47% respectively for preganglionic injury, and 91.30%, 60.00%, and 85.71% respectively for postganglionic injury.

Conclusions: The combination of STIR, balance-FFE, and DWIBS sequences can display brachial plexus pre-ganglionic and post-ganglionic injury clearly, effectively, and accurately.

MeSH Keywords: **Brachial Plexus • Magnetic Resonance Imaging • Models, Statistical**

Full-text PDF: <https://www.medscimonit.com/abstract/index/idArt/907019>

 2804

 5

 3

 16



Background

Brachial plexus is a complex neural network, formed by the anterior rami of the lower 4 cervical nerves and the first thoracic nerve (C5, C6, C7, C8, and T1), which could be divided into pre-ganglionic and post-ganglionic parts by the spinal ganglion. Traumatic brachial plexus injury is mainly caused by car accidents, occupational injuries, falling, and other accidents. Brachial plexus neuropathy can have a high morbidity by seriously affecting the motor function and sensation of upper limbs. At present, the diagnosis of brachial plexus injury is generally based on medical history, physical examination, neurological examination, and electrophysiological examination. The diagnostic accuracy is usually not satisfactory due to complex anatomical structures and varying lesion mechanisms [1,2]. Therefore, it has been a major challenge to clearly, directly, completely, and non-invasively display the brachial plexus and the related lesions with imaging methodology.

Traditional imaging methods have limitations in clinical application. In recent years, however, with the development of 3.0T magnetic resonance imaging (MRI), it has become possible to clearly display the brachial plexus root canal, which provides not only morphological information and the location of the injury, but also has a high value for clinical diagnosis [3]. Therefore, MRI is considered the preferred imaging examination method for brachial plexus injuries and related diseases [4–6].

In this study, the techniques of conventional sequences (T1WI and T2WI), short time inversion recovery (STIR), balanced fast field echo (balance-FFE), and diffusion weighted imaging with background suppression (DWIBS) were employed in brachial plexus nerve imaging. The diagnostic accuracy of 3.0T MRI in brachial plexus injury were investigated.

Material and Methods

Patients

A total of 28 patients with brachial plexus injury were enrolled from Liaocheng People's Hospital and the Third People's Hospital of Liaocheng from January 2015 to June 2016 as the brachial plexus injury group. Clinical manifestations included the shoulder and upper limb pain, numbness, amyotrophy, and dysfunction. The study protocol was approved by the Ethics Committee of Liaocheng People's Hospital and the Third People's Hospital of Liaocheng. Informed consent was obtained from every patient.

Examination methods

MRI was performed with the Philips Achieva TX 3.0T superconducting MR scanner, with a head and neck joint coil. Patients were scanned in the supine position with the head entering the scanner first. Before the examination, padding and cushions were put under the head and shoulder to make the patient comfortable and to reduce the curvature of the cervical spine. Patients were asked to reduce swallow activity and body movement during the scanning.

The MRI conventional scanning sequences of sagittal SE-T1WI (TR/TE, 2880/9.0 ms), and horizontal and sagittal FSE-T2WI (TR/TE, 3200/110 ms) were performed. The technique details involved in the pre-ganglionic scanning were: balance-FFE, for coronal scanning: TR/TE, 6.4/2.6 ms; FOV, 21 cm; layer thickness, 3.0 mm; layer spacing, 1.5 mm; number of scanning layer, 30 layers; and flip angle, 60°. Axial scanning was: TR/TE, 6.4/2.6 ms; FOV, 14 cm; layer thickness, 2.0 mm; layer spacing, 1.0 mm; number of scanning layer, 150 layers; and flip angle, 60°. The technique details involved in the post-ganglionic scanning were: STIR sequence for coronal: TR/TE, 5700/75 ms; FOV, 25 cm; layer thickness, 2.5 mm; layer spacing, 1.0 mm; number of scanning layer, 30 layers; and flip angle, 90°. DWIBS sequence of axial: FOV, 30 cm; layer thickness, 3.0 mm; layer spacing, 0; number of scanning layer, 60 layers; and flip angle, 90°. Scanning range: from upper edge of the 4th cervical vertebral body down to the lower edge of the 2nd thoracic vertebral body; from the anterior edge of the vertebral body to the posterior edge of the spinal canal. Both sides included the armpit.

Image processing and result analysis

The original images were obtained by balance-FFE, STIR, and DWIBS sequence scanning, which were imported into the Philips MR Workspace for 3D reconstruction. The maximum intensity projection (MIP), multiplanar reformation, and curved planar reconstruction (CPR) were reconstructed. The images were reviewed and analyzed by 2 senior radiologists and the images were compared to the findings which had been revealed during surgery, electromyography, or pathological examination. Signs for nerve injury mainly included the normal nerve root disappearing or interrupted, interrupted continuity, traumatic meningeal cysts, black line sign, morphological abnormality of nerve root sleeve, and thickened nerve root. Pseudo-neuroma (also known as traumatic neuroma) referred to as that which after the nerve trunk fracture, the nerve fibers continued to grow forward, and whose stump would gradually enlarge when obstructed by soft tissues and neuroma would be formed.

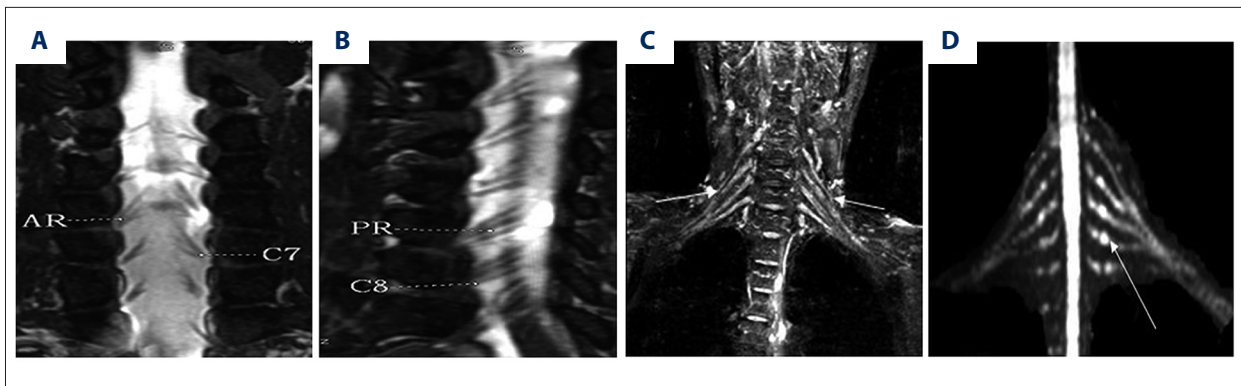


Figure 1. Images of normal brachial plexus. (A) Coronal balance-FFE, pre-ganglionic segments show filamentous signals; AR, anterior root; and C7, the seventh cervical nerve root. (B) Oblique sagittal balance-FFE images show clear signal of pre-ganglionic nerve root; PR, posterior root; and C8, the eighth cervical nerve root. (C) Coronal STIR images show strong signals of bilateral post-ganglionic nerve root of brachial plexus. (D) Coronal DWIBS images show strong signals of bilateral post-ganglionic nerve root of brachial plexus and the roundish signals of ganglion.

Table 1. Successful imaging rate of postganglionic nerves of brachial plexus by STIR sequence and DWIBS sequence.

	STIR	DWIBS	χ^2	P
Ganglion	32/50	42/50	5.197	0.023
Root	36/50	45/50	5.263	0.022
Supraclavicular nerve	40/50	43/50	0.638	0.425
Subclavian nerve	37/50	40/50	0.508	0.476

Statistical analysis

Statistical analysis was carried out with the SPSS 17.0 software (Chicago, IL, USA). The counting data were expressed as percentages and the differences were analyzed using the χ^2 test. $P < 0.05$ was considered as statistically significant.

Results

Study patients

There were 17 males and 11 females, with an average age of 27.2 ± 2.6 years (age ranging from 18 to 41 years). There were 16 cases of car accident injuries, 5 cases of machine crush injuries, 3 cases of fight injuries, and 4 cases of falling injuries. The healthy volunteer control group included 13 males and 12 females, aged 25.1 ± 2.3 years (age ranging from 20 to 38 years) with no brachial plexus injury or other brachial plexus neuropathy before examination.

MRI findings of normal brachial plexus

The pre-ganglionic nerve fibers of the brachial plexus from the 25 healthy controls were clearly imaged by balance-FFE

sequence with the successful imaging rate of 100%. The pre-ganglionic nerve fibers of the brachial plexus by balance-FFE sequence imaging showed filamentous structure (Figure 1A, 1B). The post-ganglionic nerves of the brachial plexus from healthy controls were clearly displayed in the coronal 3D reconstruction by STIR sequence or DWIBS sequence methods (Figure 1C, 1D). The post-ganglionic nerves of the brachial plexus presented round structures at the intervertebral foremen and presented striped structures at the nerve root. The successful imaging rate for the brachial plexus root and ganglion by the DWIBS sequence method was higher than by the STIR sequence method, with statistical significance ($P < 0.05$). In contrast, there was no significant difference between the 2 sequence methods in displaying the supraclavicular nerve and subclavian nerve ($P > 0.05$). The imaging results, including numbers of displayed ganglion, root, supraclavicular nerve, and subclavian nerve, are summarized in Table 1.

Traumatic brachial plexus injury

In this study, 28 cases (54 nerves) had traumatic brachial plexus injuries; 16 cases (31 nerves) had pre-ganglionic injury, and 12 cases (23 nerves) had post-ganglionic injury.

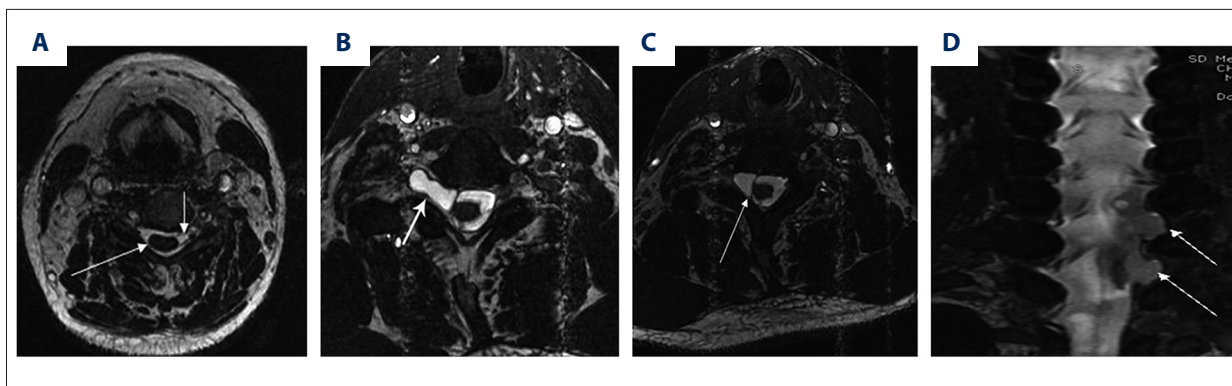


Figure 2. Images of pre-ganglionic injury of brachial plexus. (A) Axial balance-FFE image, the arrow on the right side indicates the missing low signals of nerve root. The arrow on the left side indicates the low signals of nerve root continuously spreading to the intervertebral foremen. (B) Axial balance-FFE image, the arrow indicates cerebrospinal fluid cystic aggregation and the traumatic meningeal cyst. (C) Axial balance-FFE images, arrows show the black line signs and the outside presenting meningeal cyst. (D) Coronal balance-FFE CPR images, the left side shows increased volume of C7–C8 nerve root sleeve, while low signals of nerve roots were missing.

Table 2. Types of preganglionic injury of the brachial plexus in patients revealed by MRI.

	No.	C5		C6		C7		C8		T1	
		Right	Left	Right	Left	Right	Left	Right	Left	Right	Left
Nerve root disappear or rupture	17	1	2	2	2	1	2	3	1	2	1
Nerve spreading abnormality t	10	0	1	2	1	2	0	1	2	1	0
Nerve root sleeve abnormality	4	0	0	1	0	0	1	0	1	0	1
Meningeal cyst	5	1	0	1	0	1	0	1	1	0	0
Black line sign	4	1	0	1	0	1	0	0	1	0	0

The manifestations of 16 patients with pre-ganglionic injury of the brachial plexus included 9 patients with normal nerve root disappearance (or avulsion), involving 17 nerve roots (Figure 2A). There were 10 nerve roots that could not be continuously tracked to the 5th intervertebral foramen. There were 3 patients with nerve root sleeve abnormalities involving 4 nerve root, with nerve root sleeve more obtuse compared with the healthy contralateral side (Figure 2D), and 5 traumatic cysts (Figure 2B). There were 4 patients with thickened dura matter (i.e., black line sign; Figure 2C). There was 1 patient with spinal cord edema. The details are shown in Table 2.

The manifestations of 12 patients with post-ganglionic injury of the brachial plexus included different degrees of nerve root thickening, and strong MRI signals were presented in all post-ganglionic injuries of the brachial plexus (Figure 3A); and the post-ganglionic injury involved a total of 11 nerve roots. There were 7 patients who presented interrupted nerve root continuity and disappearance of normal structures (Figure 3B, 3C), involving a total of 8 nerve roots. There were 2 patients with nerve root rigor and/or structural disorders, involving 3 nerve roots.

There was 1 patient with 1 pseudo-neuroma (Figure 3D, 3E). There were 7 patients with post-ganglionic injury presenting with soft tissue structure disorders, muscle atrophy, and edema around the damaged nerve root. The details are shown in Table 3.

The sensitivity, specificity, and accuracy of MRI examination

For the pre-ganglionic injury of the brachial plexus, a total of 43 nerve roots were examined during surgery and 38 nerve roots were confirmed to be injured. In contrast, MRI identified 31 injured nerve roots. The sensitivity of MRI detecting pre-ganglionic injury was 93.55%, the specificity was 71.43%, and the overall root accuracy was 89.47% (Table 4).

For the post-ganglionic injury of the brachial plexus, a total of 32 bundles of nerve were examined during surgery and 28 were confirmed to be injured. In contrast, MRI identified 23 bundles of injured nerve. The sensitivity of MRI detecting post-ganglionic injury was 91.30%, the specificity was 60.00%, and the overall accuracy was 85.71% (Table 5).

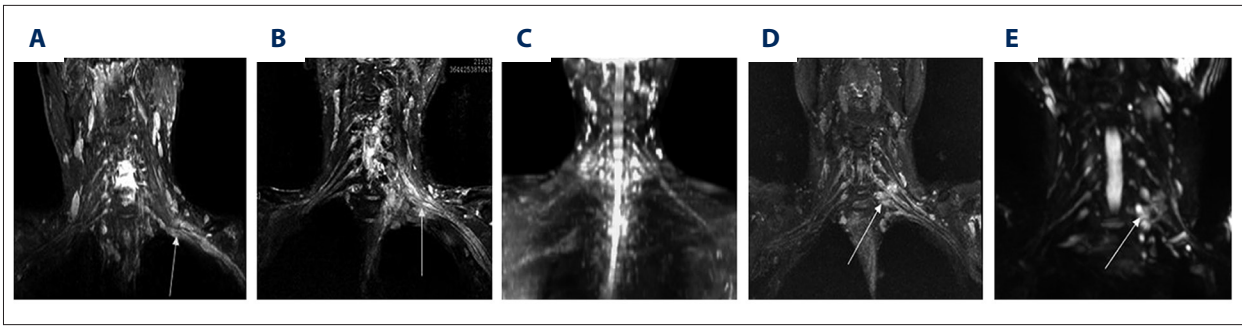


Figure 3. Images of postganglionic injury of brachial plexus. (A) MIP image of STIR sequence shows the left post-ganglionic nerve root thickening, increased signal, and rigor. (B) MIP image of STIR sequence shows disrupted continuity of the left post-ganglionic segments of the brachial plexus, structural disorder, and thickened distal end. (C) Image of DWIBS sequence shows the signals of right side subclavian brachial plexus disappeared. (D) MIP image of STIR sequence shows rupture of the left side C8 nerve root. Contracture of the ruptured segment formed pseudo-neuroma. (E) MIP image of DWIBS sequence shows C8 nerve root showing structural disorder, accompanied with nodular pseudo-neuroma formation.

Table 3. Types of postganglionic injury of the brachial plexus in patients revealed by MRI.

	No.	C5		C6		C7		C8		T1	
		Right	Left	Right	Left	Right	Left	Right	Left	Right	Left
Nerve root thickening	11	0	1	1	1	0	2	1	3	1	1
Disrupted continuity in nerve root	8	0	1	0	2	0	1	1	1	1	1
Stiffness in nerve root	3	0	0	0	0	0	1	0	1	0	1
Pseudo-neuroma	1	0	0	0	0	0	0	0	1	0	0

Table 4. Comparison between MRI (Balanced-FFE) and surgery approaches in diagnosis of preganglionic injury of brachial plexus.

	Confirmed by surgery	Excluded by surgery	Total	Sensitivity	Specificity	Accuracy
Confirmed by MRI	29	2	31	93.55%	71.43%	89.47%
Excluded by MRI	2	5	7			
Total	31	7	38	–	–	–

Table 5. Comparison between MRI (STIR and DWIBS sequences) and surgery approaches in diagnosis of the brachial plexus injury.

	Confirmed by surgery	Excluded by surgery	Total	Sensitivity	Specificity	Accuracy
Confirmed by MRI	21	2	23	91.30%	60.00%	85.71%
Excluded by MRI	2	3	5			
Total	23	5	28	–	–	–

Discussion

Sequence selection for brachial plexus scanning and its characteristics

Conventional SE (single echo) and FSE (fast spin echo) sequences are the basis of the imaging sequences. However, it is hard to distinguish the nerve from the surrounding muscle tissues using these sequences, because the signals are very similar, and high imaging quality is hard to achieve even under high contrast of the fat present. The balance-FFE sequence is a balanced steady-state free precession sequence, with short TR (repetition time) and TE (echo time), and a large deflection angle excitation. Its image has the advantages of high signal-to-noise ratio, high imaging speed, low artifacts, and good image contrast. Especially with the background contrast of cerebrospinal fluid, the multi-planar reconstruction can display improved images of preganglionic parts of the brachial plexus. The STIR sequence is based on the short T1 characteristics of adipose tissue. This technique can evenly and effectively compress the fat signal around the brachial plexus and make the brachial plexus signal predominant. The STIR sequence of thin layer can display the brachial plexus structure as continuous and clear images. Using the coronal thin slice STIR sequence, the anatomic structures and lesions in the preganglionic part of the nerve are clearly visible. DWIBS is based on STIR-EPI and diffusion weighted imaging (DWI) technology, and this technique can reduce the background signal [7]. DWIBS reduced the free water signal to the greatest extent, and therefore it cannot display the pre-ganglionic nerve root very well. However, DWIBS can well exclude the blood vessels and branches in the neck and shoulder, which has a great advantage in displaying nerve spreading. DWIBS sequences have unique advantages in displaying the brachial plexus, which is ideal for MR neural imaging [8]. Yamashita et al. [9] found that DWIBS sequence could better show the normal brachial plexus and lumbosacral plexus, while the surrounding nerves and blood vessels were hardly shown. DWIBS is not good at imaging the pre-ganglionic nerve, and it cannot be compared with other sequences in the post-ganglionic part, which is used as the first choice for diagnosing post-ganglionic injury in the brachial plexus [10]. DWIBS imaging requires shorter imaging time and higher gradient field strength, which is, however, susceptible to breathing and other motions that might lead to artifacts and uncertainty. Therefore, STIR sequence and DWIBS sequence have complementary advantages in imaging the brachial plexus.

Characteristics of normal brachial plexus images

In the balance-FFE sequence, the pre-ganglionic parts of the brachial plexus can be clearly displayed, presented as filamentous structure on the high signal contrast of cerebrospinal fluid. From the inside to the outside, the nerve roots gradually aggregate into a bundle

and gather at the intervertebral foramen, and their angles to the longitudinal axis of the spinal cord from the 5th neck nerve down to the first thoracic nerve gradually reduce. A previous study has shown that this sequence can display the pre-ganglionic nerve root with a successful rate of 100% [11]. In this study, balance-FFE sequence and the coronal joint axial scanning method were applied to obtain more valuable information. The STIR sequence and DWIBS sequence clearly displayed the post-ganglionic parts of the brachial plexus. After CPR and MIP treatment, the post-ganglionic parts of the brachial plexus were displayed in continuity on the same layer. Normal post-ganglionic ganglion displayed strong round signals at the intervertebral foramen and striped signals at the nerve roots. Comparison in the displaying performance between DWIBS and STIR sequences showed that DWIBS was superior to STIR in displaying post-ganglionic segments of the brachial plexus (nerve root and ganglion), while not superior in displaying supraclavicular nerve and subclavian nerve. The combination of DWIBS and STIR sequences can provide more valuable information.

Characteristics of traumatic brachial plexus injury

The characteristics of MRIs of the pre-ganglionic injury of the brachial plexus includes disappearance or discontinuation of the normal nerve root. The structures with filamentous signals disappeared or were unclear on the high contrast background of the cerebrospinal fluid. The injury could be clearly displayed by images obtained from coronal or axial balance-FFE sequences. This type of injury involved 17 pre-ganglionic nerve segments (54.84%), and all from patients who suffered severe brachial plexus injury. In addition, the nerve roots were with rigor, or could not be tracked to the intervertebral foramen. Meanwhile, in contrast to the contralateral side, the filaments were significantly reduced on imaging. This type of injury involved 5 patients with 10 nerve roots (32.26%). There was a total of 5 traumatic meningeal cysts found. However, meningeal cysts are not unique in brachial plexus injury. For some patients with meningeal cysts, no nerve injury was found during surgery. We also found thickened dura matter (i.e., black line sign) in 4 patients. This type of injury is common in pre-ganglionic injury of the brachial plexus, and often occurs simultaneously with traumatic meningeal cysts, manifested as striped signal (i.e., black line sign) between the meningeal cyst and normal subarachnoid space. Not all of cysts are accompanied with thickened dura matter, and the co-occurrence may be related to the injury degree [12,13]. We found nerve root sleeve abnormalities in 3 patients involving 4 nerve roots (12.90%), which showed characteristics of increased volume when compared to the contralateral side, with the ends extended outwards. This type of injury may be related to scar formation after nerve root sleeve avulsion. We also found injury of spinal cord edema, deformation, and displacement in 1 patient. Hayashi et al. [14] found that spinal cord injury often suggests pre-ganglionic injury, and the factors that might cause spinal cord deformation

(or shift) are generally structural abnormalities in the spinal canal, which compress or pull the spinal cord.

MRI (STIR, DWIRS) is the one of the appropriate methods used to show the normal post-ganglionic nerve. The characteristics of MRI in our study of post-ganglionic injury of the brachial plexus included the complete nerve rupture manifested as the interrupted continuity and retraction of distal end (7 patients with 8 nerve roots, 34.78%); or thickened nerve accompanied with increased signals caused by increasing water content in tissues under edema and inflammation (9 patients with 11 nerves, 47.82%; all injuries had occurred within 1 month). We also found nerve cord structural disorder or rigor. These features are often presented in the late stage of brachial plexus injury when the nerves were not completely ruptured, resulting in local nerve hemorrhage and fibrosis. There were 2 patients with 3 nerves presenting with this type of injury; these injuries had occurred within 1–2 years. There was 1 case (4.34%) of pseudo-neuroma detected, caused by contracture of the ruptured nerve segments. The soft tissue edema around the damaged nerve presenting disrupted structure, increased signals, and muscle atrophy. Overtime, muscle atrophy could develop due to loss of nerves. This type of post-ganglionic injury was observed in 7 patients. Our study results showed that post-ganglionic injury of the brachial plexus was closely related to the MRI features. Experts have suggested that the most common MRI characteristics in post-ganglionic injury of the brachial plexus were nerve stem thickening and increased signals, accounting for about 41% of post-ganglionic injury [15]. Our results of 47.82% were in line with this other study result. It has been reported that mixed injury of the brachial plexus is

often more severe and is accompanied by both pre-ganglionic injury and post-ganglionic injury [16]. However, in our study, mixed brachial plexus injury was not identified.

The sensitivity, specificity, and accuracy of MRI examination on brachial plexus injury

Based on the results obtained in our study, MRI identifying pre-ganglionic and/or post-ganglionic injury of the brachial plexus and showed high sensitivity (>90%) but low specificity. Therefore, the gold standard for brachial plexus injury diagnosis should be through surgery. However, due to the difficulty of surgery, the lesion diagnosis in some patients has been made by intraoperative electrophysiological results, which could induce bias in analyzing the specificity of MRI. Considering the limited sample size in this study, future studies are still needed to clarify the value of MRI in brachial plexus injury diagnosis.

Conclusions

The combination of MRI conventional sequence and balance-FFE, STIR, and DWIRS sequence represent an ideal imaging methodology for brachial plexus diseases. This combination can provide accurate and reliable information about the location and degree of the brachial plexus injury, and can facilitate early treatment, improve prognosis, and reduce disabilities in the clinic.

Conflicts of interest

None.

References:

1. Tomura N, Saginoya T, Kokubun M et al: T2-weighted IDEALfast spin echo imaging of the braehial plexus: Comparison withSTIR. *Acta Radiologica*, 2015; 56: 1242–47
2. Martín Noguerol T, Barousse R, Socolovsky M, Luna A: Quantitative magnetic resonance (MR) neurography for evaluation of peripheral nerves and plexus injuries. *Quant Imaging Med Surg*, 2017; 7: 398–421
3. Chanlalit C, Vipulakorn K, Jirattanapochai K, Mairiang E: Value of clinical findings, electrodiagnosis and magnetic resonance imaging in the diagnosis of root lesions in traumatic brachial plexus injuries. *J Med Assoc Thai*, 2005; 88: 66–70
4. Somashekar D, Yang LJS, Ibrahim M et al: High-resolution MRlevaluation of neonatal brachial plexus palsy: A promising alternative to traditional CT myelography. *Am J Neuroradiol*, 2014; 35(6): 1209–13
5. Upadhyaya V, Upadhyaya DN, Kumar A et al: MR neurography in traumatic braehial plexopathy. *Eur J Radial*, 2015; 84: 927–32
6. Wade RG, Itte V, Rankine JJ et al: The diagnostic accuracy of 1.5T magnetic resonance imaging for detecting root avulsions in traumatic adult brachial plexus injuries. *J Hand Surg Eur Vol*, 2018; 43: 250–58
7. Takahara T, Imai Y, Yamashita T et al: Diffusion weighted whole body imaging with background body signal suppression (DWIBS): Technical improvement using free breathing, STIR and high resolution 3D display. *Radiat Med*, 2004; 22: 275–82
8. Gao L, Liang B, Zhang B: [Application of background signal suppression diffusion weighted imaging in brachial plexus imaging diagnosis.] *Z Sun Yat-Sen University Xue Bao (Medical Science)*, 2007; 28: 322–26 [in Chinese]
9. Yamashita T, Kwee TC, Takahara T: Whole-body magnetic resonance neurography. *N Engl J Med*, 2009; 361: 538–39
10. Takahara T, Hendrikse J, Yamashita T et al: Diffusion-weighted MR neurography of the brachial plexus: Feasibility study. *Radiology*, 2008; 249: 653–60
11. Yoneyama M, Takahara T, Kwee TC et al: Rapid highresolution MR neurography with a diffusion-weightedpre-pulse. *Magn Reson Med Sci*, 2013; 12: 111–19
12. Qin BG, Yang JT, Yang Y et al: Diagnostic value and surgical implications of the 3D DW-SSFP MRI on the management of patients with brachial plexus injuries. *Sci Rep*, 2016; 6: 35999
13. Yang J, Qin B, Fu G et al: Modified pathological classification of brachial plexus root injury and its MR imaging characteristics. *J Reconstr Microsurg*, 2014; 30: 171–78
14. Hayashi N, Masumoto T, Abe O et al: Accuracy of abnormal paraspinale muscle findings on contrast-enhanced MR images as indirect signs of unilateral cervical root-avulsion injury. *Radiology*, 2002; 223: 397–402
15. Chhabra A, Madhuranthakam AJ, Andreisek G: Magnetic resonance neurography: Current perspectives and literature review. *Eur Radiol*, 2018; 28(2): 698–707
16. Geng M, Wang G, Liu Y et al: [The value of 3.0T MRI in the diagnosis of brachial plexus injury.] *Chinese Imaging Journal of Integrated Traditional and Western Medicine*, 2010; 489–92, 515 [in Chinese]